

Research paper

Selected herbicides screened for toxicity and analysed as inhibitors of both cholinesterases



Vesna Pehar ^{a,1}, Dora Kolić ^{b,1}, Antonio Zandona ^b, Goran Šinko ^b, Maja Katalinić ^b, Višnja Stepanić ^{c, **}, Zrinka Kovarik ^{b,*}

^a Croatian Defense Academy "Dr. Franjo Tuđman", Ilica 256b, 10000, Zagreb, Croatia

^b Institute for Medical Research and Occupational Health, Ksaverska cesta 2, 10000, Zagreb, Croatia

^c Ruder Bošković Institute, Bijenička 54, HR-10002, Zagreb, Croatia

ARTICLE INFO

Keywords:

Acetylcholinesterase
Butamifos
Cytotoxicity
Glyphosate
Neurotoxicity
Organophosphates pesticides

ABSTRACT

Sets of 346 herbicides in use and 163 no longer in use were collected from open access online sources and compared *in silico* with cholinesterases inhibitors (ChI) and drugs in terms of physicochemical profile and estimated toxic effects on human health. The screening revealed at least one potential adverse consequence for each herbicide class assigned according to their mode of action on weeds. The classes with most toxic warnings were K1, K3/N, F1 and E. The selection of 11 commercial herbicides for *in vitro* biological tests on human acetylcholinesterase (AChE) and butyrylcholinesterase (BChE), the enzymes involved in neurotoxicity and detoxification of various xenobiotics, respectively, was based mainly on the structural similarity with inhibitors of cholinesterases. Organophosphate anilofos and oxyacetanilide flufenacet were the most potent inhibitors of AChE (25 µM) and BChE (6.4 µM), respectively. Glyphosate, oxadiazon, tembotrione and terbutylazine were poor inhibitors with an estimated IC₅₀ above 100 µM, while for glyphosate the IC₅₀ was above 1 mM. Generally, all of the selected herbicides inhibited with a slight preference towards BChE. Cytotoxicity assays showed that anilofos, bensulide, butamifos, piperophos and oxadiazon were cytotoxic for hepatocytes (HepG2) and neuroblastoma cell line (SH-SY5Y). Time-independent cytotoxicity accompanied with induction of reactive oxygen species indicated rapid cell death in few hours. Our results based on *in silico* and *in vitro* analyses give insight into the potential toxic outcome of herbicides in use and can be applied in the design of new molecules with a less impact on humans and the environment.

1. Introduction

Herbicides are pesticides used for the selective destruction of weeds by inhibiting or interrupting their growth and development. Although herbicides are mainly utilized for agricultural purposes, they are also extensively applied in industrial or public sites such as irrigation canals, roadsides, fence lines, recreational areas, lawns, gardens, ponds and lakes [1,2]. Herbicides are classified according to their weed specificity, chemical structure, time of application and mode of action [2–6]. They target specific plant metabolic pathways such as photosynthesis, biosynthesis of amino acids, lipids and pigments, plant hormone action or regulation of cell division [3,6]. To facilitate the use of herbicide rotation and mixtures as a strategy to combat weed resistance, a

classification system was created by the global Herbicide Resistance Action Committee (HRAC), an international body founded by the agrochemical industry that helps to protect crop yields and quality worldwide [7]. According to the Food and Agriculture Organization of the United Nations (FAO) [8], the application of herbicides, as well as other pesticides like insecticides and fungicides, increased by nearly 50% between the 1990s and 2020, with increases in the share of total pesticides coming mainly from herbicides (from 41% to 52%). While the Americas experienced the highest growth rates in total pesticide use since the 1990s, Europe on the other hand increased pesticides use in agriculture by just 3%, most likely due to the stringent European Common Agricultural Policy put in place, which monitors and controls the pesticide use [8]. Moreover, obsolete pesticides still present a risk as

* Corresponding author.

** Corresponding author.

E-mail addresses: vismja.stepanic@irb.hr (V. Stepanić), zkovarik@imi.hr (Z. Kovarik).

¹ Equally contributed authors.

they are stored in the developing regions of Asia, Latin America, and Africa [9]. In recent years, obsolete organochlorine pesticides have been increasingly replaced with more effective and safer alternatives with faster biodegradation rates such as organophosphorus pesticides and neonicotinoids. However, some can still affect non-target species via water, soil, and contaminated plant tissues [10]. Nevertheless, the desired property of pesticides is target selectivity, and herbicides are frequently claimed to be low toxic for non-targeted organisms, since their modes of action assumingly concern only specific plant metabolic pathways [2,11]. Mostafalou and Abdollahi [12] systematically reviewed recorded evidences of various malignant, neurodegenerative, respiratory, reproductive, developmental, and metabolic diseases in relation to different routes of human exposure to pesticides. Carcinogenicity is the most studied and reported toxicity for each group of pesticides. However, in addition to insecticides, herbicides have also been linked to the occurrence of neurodegenerative diseases [12].

Today's common models for the evaluation of hazardous effects of herbicides are *Tetrahymena pyriformis*, *Daphnia* species and goldfish (*Carassius auratus*) [2,13–15]. *D. magna* has been used as a model organism for investigating cardiac activity of small compounds (such as acetylcholine, tetraethyl pyrophosphate, pilocarpine, adrenaline and rotenone) [16] and assessing the effects of short-term exposure to chemicals that alter monoamine signalling [17]. The protozoan *T. pyriformis* has been used as a unicellular model to explore chemotactic effects of human neurotransmitters [18] because it has binding sites for some of these molecules at its membrane. Tetrahymena also produces the neurotransmitters dopamine, adrenaline, noradrenaline, and catecholamine and the level of these neurotransmitters can be used as a biomarker for assessing neurotoxicity and detecting possible toxicants, responsible for dopaminergic disorders related to human neurological and psychological diseases [13,19].

Many pesticides are organophosphorus compounds (OP), which are known as potent inhibitors of acetylcholinesterase (AChE) and butyrylcholinesterase (BChE) due to the phosphorylation of their catalytic sites [20]. Both enzymes can be found in synapses of the central nervous system (CNS), neuromuscular junctions of the peripheral nervous system and in blood where AChE is bound to the erythrocyte membrane and BChE dissolved in plasma [21]. OP can exert their neurotoxic effect by inhibiting AChE, an essential enzyme for neurotransmitter acetylcholine hydrolysis [22]. AChE inhibition leads to the accumulation of acetylcholine in synapses and causes overstimulation of cholinergic receptors which may induce a plethora of symptoms, including miosis, bronchorrhea, bradycardia, excessive salivation, convulsions and in severe poisoning cases loss of consciousness, respiratory failure and cardiac arrest [23,24]. Though BChE is not as physiologically relevant as AChE, BChE hydrolyses various drugs and xenobiotics and serves as bio-scavenger in cases of poisoning by highly toxic anti-AChE compounds [25–27].

As mentioned previously, most herbicides exert their mode of action in weeds via pathways not found in humans and therefore their general or neurotoxic mechanisms were mainly studied on non-target organisms and rarely on mammals [11]. Herein we carried out an extensive *in silico* screening of a library of 346 commercially available herbicides and 163 obsolete ones, collected from publicly available online databases and the literature, to identify possible toxic effects on human health. Based on the structural and/or physicochemical similarity with the known cholinesterase inhibitors (ChIs) we selected 11 herbicides in use. We report here the *in vitro* analysis of their kinetics of AChE and BChE inhibition, molecular docking studies, and evaluation of their cytotoxic profiles on two cell lines, hepatocytes (HepG2) and neuroblastoma (SH-SY5Y).

2. Material and methods

2.1. *In silico profiling of herbicides*

A dataset of 509 herbicides was formed from two sets of herbicides. The dataset of 346 commercially available herbicides was downloaded from HRAC online resources [6]. The other dataset contains 163 outdated herbicides collected from the literature and open-source online databases: Compendium of Pesticide Common Names [28], Pesticide Properties Database (PPDB) [29], PubChem database [30] and Pesticide Target Interaction Database (PTID) [31]. The set of 68 cholinesterase inhibitors (ChI) was also downloaded from PubChem database. The set of 2503 approved drugs was collected from ChEMBL database [32].

Physicochemical and ADME/Tox parameters of compounds were computed by ADMET software Predictor™ 9.0 (Simulations Plus Inc., USA) [33] and DataWarrior [34]. For the purpose of analysis of similarity between herbicides and ChI, the compounds were represented by the structural ECFP6 fingerprints (features present in more than four molecules were taken into account) [35] and described by physicochemical features relevant for the CNS activity [36]. The analyses were carried out by two methods: principal component analysis (PCA) and t-distributed stochastic neighbour embedding (t-SNE). t-SNE analysis was done with the following values of tuneable parameters: perplexity 30, eta (rate learning) 300 and 5000 iterations. The ECFP6 fingerprints and Jaccard index (=1-Tanimoto coefficient) as a structural similarity measure as well as the PCA and t-SNE similarity analyses were calculated by R packages rcdk, stats (the function *prcomp*) and Rtsne, respectively. The R computing was done within RStudio (R version 3.6.3) environment [37].

The predicted values for a panel of toxicity and physicochemical parameters relevant for neurotoxic and developmental impact, along with structural similarity with known inhibitors of primarily AChE were used for selection of herbicides for *in vitro* testing.

2.2. *Selected herbicides, chemicals and enzymes*

All herbicides were analytical grade with declaration of purity between 98.3% and 99.9% (Sigma-Aldrich, USA). Majority of the herbicides were purchased, while glyphosate, tembotrione and terbutylazine were generous gifts from Dr Davor Želježić and Dr Vilena Kašuba (Institute for Medical Research and Occupational Health, Zagreb, Croatia). Stock solutions (10 mM) were made in isopropyl alcohol and were stored at 4 °C. Further dilutions were made in isopropyl alcohol for the IC₅₀ evaluation and in methanol for progressive inhibition. Glyphosate was dissolved and diluted in water.

Acetylthiocholine iodide (ATCh), thiol reagent 5,5'-dithiobis(2-nitrobenzoic acid) (DTNB) and bovine serum albumin (BSA) were purchased from Sigma-Aldrich, USA. Stock solution of ATCh was prepared in water and DTNB was prepared in sodium phosphate buffer (0.1 M, pH 7.4). The final concentrations of ATCh and DTNB for all measurements were 1 mM and 0.3 mM, respectively.

Recombinant human AChE and purified human plasma BChE were a generous gift from Dr Xavier Brazzolotto and Dr Florian Nachon (*Département de Toxicologie et Risques Chimiques, Institut de Recherche Biomédicale des Armées*, Bretigny-sur-Orge, France). Enzymes were stored at 4 °C.

2.3. *Inhibition of cholinesterases by herbicides*

AChE and BChE activity was measured in the presence of herbicides within a range of concentrations (0.1 µM - 1 mM). The inhibition mixture contained phosphate buffer (0.1 M, pH 7.4), DTNB, enzyme and herbicide. The concentration of AChE and BChE was 4 ng/mL and 28 ng/mL in the inhibition mixture, respectively. After 30 min of incubation residual enzyme activity was measured upon addition of ATCh (50 µL ad 1 mL) using Ellman method [38] at 25 °C and 412 nm on a CARY 300

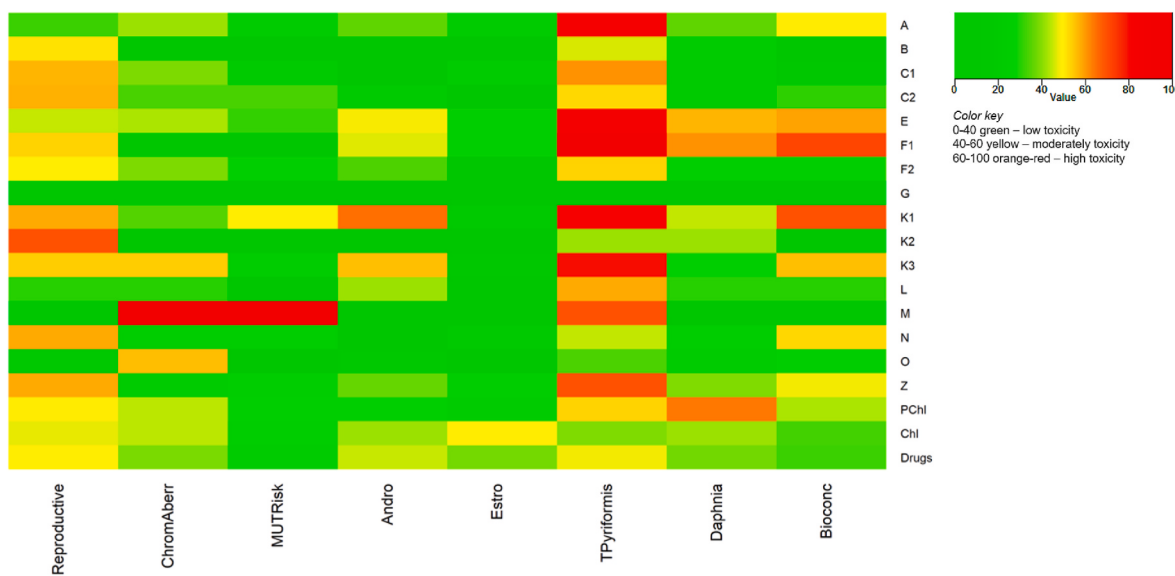


Fig. 1. Heat map of toxicity parameters in terms of % of toxic compounds predicted out of 346 commercial herbicides sorted by legacy HRAC classification system, 68 cholinesterase inhibitors (PChl and non-OP Chl) and more than 2000 approved drugs as denoted on the y-axis. The x-axis presents estimated human toxicities: reproductive/developmental toxicity (*Reproductive*), chromosomal aberration (*ChromAberr*), mutagenicity by Ames test (*MUT Risk*), rat androgen receptor affinity (*Andro*), rat estrogen receptor affinity (*Estro*), toxicity on *T. pyriformis* (*Tpyriformis*) and *D. magna* (*Daphnia*) as well as bioconcentration factor for uptake (*Bioconc*).

spectrophotometer (Varian Inc., Australia) with a temperature controller. Absorption measurements lasted up to 2 min. Due to poor solubility in phosphate buffer, herbicides dissolved in isopropyl alcohol were tested up to 100 μ M. Additionally, isopropyl alcohol significantly inhibited the enzyme activity above 5% v/v. The IC₅₀ values were determined from at least three experiments by a nonlinear fit of the herbicide concentration logarithm values vs. % of enzyme activity using Prism 9 software (GraphPad, San Diego, USA).

For progressive inhibition, AChE and BChE were incubated up to 7 h with OP herbicides anilofos, bensulide, butamifos and piperophos (1–150 μ M) in a mixture of buffer and DTNB. Enzyme activity was measured at designated times upon addition of ATCh using the Ellman method [38]. Control samples contained solvents isopropyl alcohol and methanol instead of a herbicide. Methanol improved solubility and was a less potent inhibitor of the enzymes, especially AChE, compared to isopropyl alcohol. In the final inhibition mixture, methanol was 8.5–9.99% v/v, while isopropyl alcohol was 0.01–1.5% v/v. The inhibition rate constants at a given herbicide concentration (k_{obs}) were calculated by linear regression according to a previous study [39] or by two-phase decay equation [40]. For inhibition of BChE by butamifos, the first-order inhibition constant (k_{max}), enzyme-inhibitor equilibrium dissociation constant (K_i) and the overall second-order rate constant of inhibition (k_i) were evaluated as described previously [41] using Prism 9 software (GraphPad, San Diego, USA).

2.4. Molecular modelling of interactions of cholinesterases with herbicides

The 3D structures of herbicides for molecular docking were determined by optimization with the MMFF94 force field using ChemBio3D Ultra 12.0 (PerkinElmer, Inc., Waltham, MA, USA). The Discovery Studio 20.1 (BioVia, San Diego, CA, USA) Dock Ligands protocol (CDOCKER) with a CHARMM force field was used for the docking study of herbicides in the active site of human AChE and BChE [42,43]. We used crystal structures of human AChE PDB code 4PQE [44] and BChE PDB code 2PM8 [45]. The binding site within the AChE or BChE was defined as the largest cavity in the enzyme structure surrounded by a sphere with 13 Å radius and it was used as the rigid receptor [46]. Details about ligand docking using the CDOCKER protocol and afterward scoring of generated ligand poses by a CHARMM energy were described

previously [46,47].

2.5. Cells

Human neuroblastoma SH-SY5Y (ECACC 94030304) and human Caucasian hepatocyte carcinoma HepG2 (ECACC 85011430) cells were obtained from the certified cell-bank The European Collection of Authenticated Cell Cultures (ECACC). SH-SY5Y cells were grown in DMEM F12 medium supplemented with 15% v/v fetal bovine serum (FBS), 2 mM glutamine, 1% v/v Penicillin/streptomycin (PenStrep) and 1% v/v non-essential amino acids (NEAA). HepG2 cells were grown in EMEM medium supplemented with 10% v/v FBS, 2 mM glutamine, 1% v/v PenStrep and 1% v/v NEAA. All media and supplements were purchased from Sigma-Aldrich, Steinheim, Germany. All cells were maintained at 37 °C in 5% CO₂-enriched air at saturation humidity, the medium was changed every two to three days, and passages were performed according to standard protocol [48]. Phosphate-buffered saline (PBS, pH 7.4) was prepared according to a standard recipe [49] and used for washing the cells when needed in the assays.

2.6. Cytotoxicity screening

The cytotoxic profile of tested herbicides was determined by measuring the succinate dehydrogenase mitochondrial activity of exposed cells [50]. For this purpose, we used the commercially available MTS detection reagent assay (CellTiter 96® AQueous One Solution Cell Proliferation Assay, Promega, Madison, WI, USA). The procedure followed a previously described protocol [51] and the effect was determined after 1, 4, 24 and 48 h exposure to herbicides (0.01–100 μ M). Staurosporine (3 μ M; Abcam, Cambridge, UK) was used as a positive control. Data was evaluated as a percentage of the observed inhibition of cell viability in treated samples compared to control untreated cells from at least two independent experiments (performed in duplicate or triplicate). IC₅₀ (concentration of herbicide that inhibited 50% of the cells) was calculated by Prism 9 software (GraphPad, San Diego, USA).

2.7. Oxidative status

Induction of reactive oxygen species (ROS) by herbicides was

Table 1

Physicochemical parameters^a relevant for CNS activity, calculated for 346 herbicides of different herbicidal modes of action with more than two members [6]. The threshold values for molecular properties relevant for CNS activity are listed in the last row [36].

HRAC classes ^b	MW	TPSA/Å ²	HBD	HBA	RB	logP	logD	BBB_Filter/%	logBB
A (1) [21]	353 ± 44	65.8 ± 9.3	1	5	6	3.67 ± 0.71	2.27 ± 1.53	62	-0.60 ± 0.38
B (2) [57]	403 ± 64	136 ± 30	1	10	7	1.70 ± 0.79	-0.55 ± 1.33	30	-0.97 ± 0.32
C1 (5) [42]	242 ± 29	68.6 ± 13.2	2	5	5	2.56 ± 0.91	2.41 ± 1.29	57	0.14 ± 0.40
C2 (5) [29]	247 ± 47	43.7 ± 16.0	1	4	4	2.64 ± 0.90	2.64 ± 0.90	100	0.15 ± 0.35
C3 (6) [5]	346 ± 88	67.3 ± 36.2	1	4	1	3.52 ± 1.74	2.20 ± 2.49	80	-0.12 ± 0.68
D (22) [4]	252 ± 144	21.6 ± 30.2	0	0	0	-4.80 ± 1.92	-4.80 ± 1.92	75	-1.19 ± 0.22
E (14) [28]	366 ± 56	74.7 ± 22.3	0	5	3	3.60 ± 1.00	2.92 ± 1.66	86	0.10 ± 0.69
F1 (12) [7]	344 ± 33	38.3 ± 12.9	1	3	3	3.91 ± 0.79	3.92 ± 0.79	100	0.51 ± 0.19
F2 (27) [14]	405 ± 47	91.0 ± 22.5	0	5.5	3	2.45 ± 1.39	1.65 ± 1.94	79	-0.68 ± 0.73
K1 (3) [18]	331 ± 36	89.5 ± 33.5	0.5	5	6	4.10 ± 0.73	3.85 ± 1.46	100	0.66 ± 0.30
K2 (23) [6]	222 ± 26	43.2 ± 11.9	1	3	4.5	2.78 ± 0.69	2.78 ± 0.69	100	0.31 ± 0.20
K3 (15) [29]	306 ± 55	39.0 ± 19.1	0	3	6	3.22 ± 0.96	3.10 ± 1.25	97	0.11 ± 0.37
L (29) [6]	301 ± 103	61.5 ± 28.7	1	5	4	3.38 ± 0.78	3.38 ± 0.78	67	-0.21 ± 0.46
M (24) [6]	238 ± 21	113 ± 4	1	5	1.5	3.16 ± 0.74	0.64 ± 1.13	100	-0.05 ± 0.12
N (15) [18]	232 ± 61	29.7 ± 15.4	0	2	6	3.10 ± 0.96	2.61 ± 2.00	100	0.05 ± 0.59
O (4) [24]	243 ± 41	56.8 ± 16.8	1	3	2.5	2.55 ± 0.88	-0.04 ± 1.12	58	-0.58 ± 0.32
Z (0) [19]	277 ± 63	42.2 ± 21.5	1	3	5	3.12 ± 1.58	2.51 ± 2.02	100	0.01 ± 0.50
Thresholds	<450	<60-70	<3	<7	<8	<5	<5	>0	

^a Molecular weight (MW), topological polar surface area (TPSA), number of hydrogen bond donor (HBD), hydrogen bond acceptor (HBA), and rotatable bonds (RB), lipophilicity coefficient (n-octanol/water) (logP), distribution coefficient (log D), % of molecules in a HRAC class predicted to cross blood-brain barrier (BBB_Filter), and blood-brain barrier retention (logBB). MW, TPSA, logP, logD, and logBB are given mean ± standard deviation. HBD/HBA and RB values are medians.

^b The letters denote legacy HRAC classification system, numbers in parentheses correspond to the 2020 global HRAC classification system in which the N and K3 classes are merged, and the number in square brackets is the number of herbicides for a given legacy HRAC class.

determined using a cell-permeable reagent 2',7'-dichlorofluorescin diacetate dye (DCFDA) and cell-permeable reagent monochlorobimane (mCB) for quantifying intracellular glutathione (GSH) levels. The procedure followed a previously described protocol [51]. Hydrogen peroxide (H₂O₂) or *tert*-butyl hydroperoxide (tBOOH), both 100 µM final concentrations, were used as a positive control. All chemicals were purchased from Sigma-Aldrich, Steinheim, Germany. Data was evaluated from at least two independent experiments (performed in duplicate) using Prism 9 software (GraphPad, San Diego, USA) and presented as a normalized signal to the untreated control, according to the manufacturer's calculation protocol.

3. Results and discussion

3.1. In silico toxicity profiling of herbicides

The qualitative toxicity profile of herbicides, sorted by legacy HRAC classification, is illustrated as a heat map in Fig. 1. The heat map was obtained by analysis of outputs of ADMET Predictor models for reproductive/developmental toxicity and genotoxicity, rodent and human toxicity as well as ecotoxicity. The model outputs are qualitative (the two classes: toxic and non-toxic) or are transformed into classes by using pre-defined toxicity cut-offs. According to the two-class ADMET Predictor models for assessing a compound's likelihood of binding to rat estrogen (*Estro*, Fig. 1) or androgen (*Andro*) receptors, most of the commercial herbicides are not predicted to cause endocrine disruption via interference with the binding of estrogenic hormones and modification of downstream signalling, but several herbicides (particularly from classes K1 and K3) are estimated to have antiandrogen activity. The majority of herbicides are also qualitatively estimated to have a relatively low risk of causing genotoxicity through triggering chromosomal aberrations (two-class trait *ChromAber*) and mutagenicity (trait *MUTRisk* ≥ 1.5). However, the analysis pointed to a potential reproductive/developmental toxicity (two-class *Reproductive*) and growth inhibition toxicity on *Tetrahymena pyriformis* (*Tpyriformis*, 50% inhibition growth concentration after ~40 h of exposure, pIGC₅₀ [mM] ≥ 1), particularly for those herbicides with the following targeted biological processes in weeds: inhibition of fatty acid synthesis – classes A and K3, inhibition of chlorophyll heme synthesis – the class E, inhibition of carotenoid synthesis – the class F1, and inhibition of microtubule assembly – the class

K1, and the class Z. For the sake of reference, we included a group of 68 ChI and a set of 2503 approved drugs into the toxicity profiling analysis, as well as predictions for *Daphnia magna* (water flea), another frequently employed model for acute toxicity (lethal toxicity after 48 h of exposure, LC₅₀ [mg/L] ≤ 0.3). In comparison with ChI and drugs, these herbicides could have considerably higher potential to cause *T. pyriformis* growth inhibition. On the other hand, OP ChI could be prone to cause *Daphnia magna* death. According to analysis, drugs are safe molecules, as expected. Bioaccumulation as a ratio of the chemical concentration in organism (fish) to that in a water environment is considered as a parameter for estimating tissue uptake and risk of chronic poisoning. The strong accumulation (*Bioconc* > 25) is predicted for the herbicides belonging to classes F1 (85.7%), K1 (83.3%), E (67.9%), and K3 (62.1%).

Commercially available herbicides were further compared with 163 obsolete herbicides (Figs. S1 and S2). The comparison revealed that commercial herbicides were significantly less toxic than obsolete herbicides concerning chromosomal aberrations and bioaccumulation (Fig. S2). Reduction of these two toxicities may be a result of the optimization of ADME properties in a modernized process of designing novel herbicides. Overall, our *in silico* toxicity screening highlights reproductive/developmental toxicity and growth inhibitory effects on *T. pyriformis* as the most common biological issue of herbicides. For each class there is at least one potential toxicity warning, while the classes with multiple warnings are K1, K3, M, F1, E, and C1.

3.2. In silico CNS-penetration ability of herbicides

Herbicides were characterised in terms of physicochemical properties commonly used to assess the ability of the compounds to cross the blood-brain barrier (BBB) and thus to have a CNS activity [36] (Tables 1 and S1): lipophilicity coefficient (logP), distribution coefficient at pH 7.4 (logD), topological polar surface area (TPSA), molecular weight (MW), number of hydrogen bond accepting/donating atoms (HBA/HBD) and number of rotatable bonds (RB). The two parameters calculated by the ADMET Predictor models, qualitative likelihood (high/low) of crossing BBB (BBB_Filter denotes % of molecules per class predicted to pass BBB) and retention in the brain once taken up (logBB), were also included in this analysis. Classes of herbicides predicted to have adverse effects on human health (Fig. 1), particularly those in

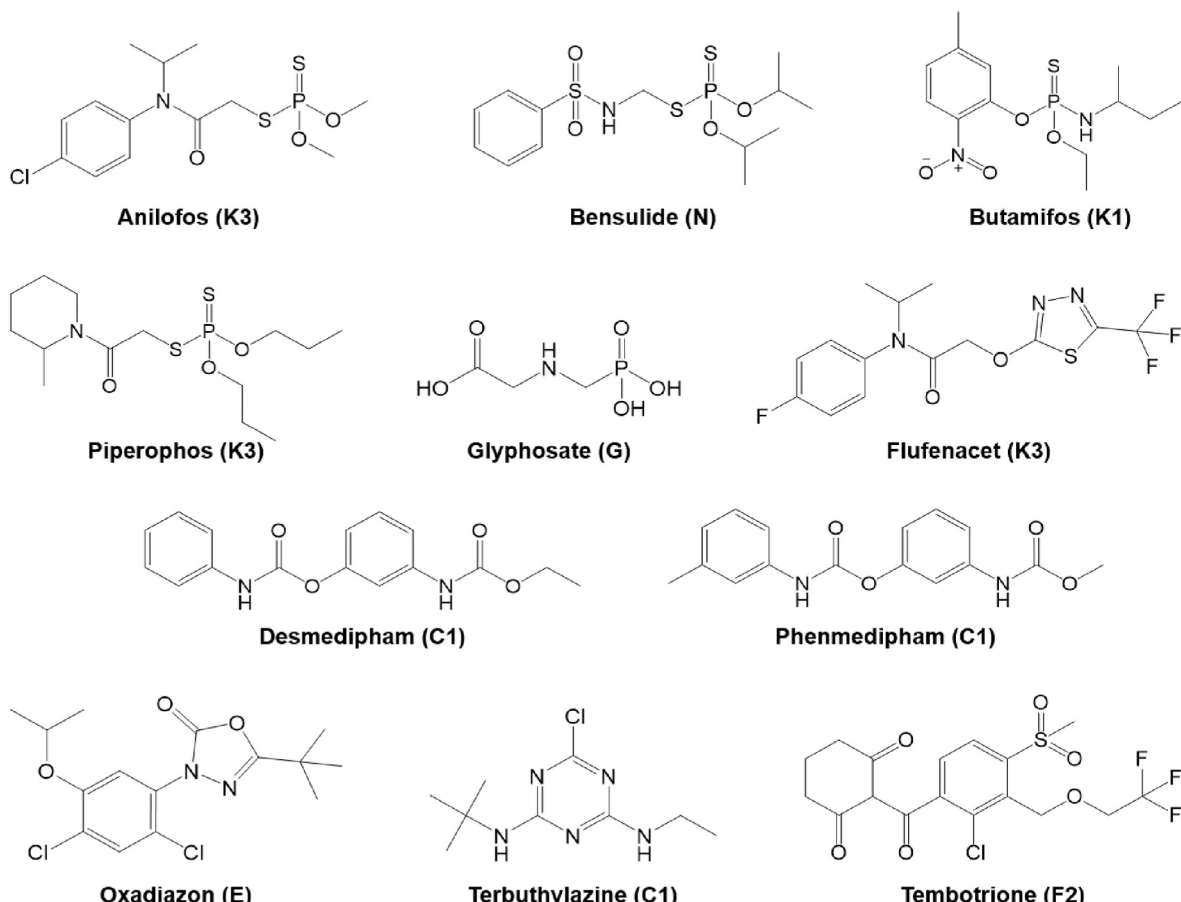


Fig. 2. Chemical structures and corresponding legacy HRAC classes of eleven commercially available herbicides chosen for biological studies: organophosphates (anilofos, bensulide, butamifos, piperophos, and glyphosate), oxyacetanilide (flufenacet), carbamates (desmedipham and phenmedipham), oxadiazolone (oxadiazon), triazine (terbutylazine) and triketone (tembotrione).

subgroups F1 and K3, also have an average physicochemical profile favourable for CNS-active compounds, which may contribute to the hypothesis of their toxic effects (Table 1). These herbicides and N class herbicides are generally nonpolar (low TPSA) and nonionizable small molecules with logP values between 2.5 and 5, and low number of HBD atoms. The mean and median values of the seven calculated parameters for these classes satisfy most of the seven rules listed in the last row of Table 1. In addition, it was predicted that a significant proportion of these herbicides (*BBB_Filter*) would pass the BBB and remain in the brain (positive *logBB* values). For comparison, C1 herbicides are somewhat more polar and have a considerable number of HBD atoms, while herbicides from class B are generally polar molecules with relatively numerous HBD and HBA atoms. Hence, these herbicides are predicted to have an unfavourable physicochemical profile for achieving significant brain exposure by passive transport. Obsolete herbicides have similar physicochemical profiles as commercial herbicides from respective classes (Table S1).

3.3. Selection of potential cholinesterase inhibitors

The OP herbicides were selected for *in vitro* screening based on their structural similarity with ChI as it is evident from the t-SNE plot, and physicochemical properties *i.e.* potential CNS-activity (Fig. 3 and Table S2). Additionally, toxicity parameters of the selected herbicides used for the generation of the heat maps are listed in Table S3. The t-SNE plot was generated using structural fingerprint descriptors for 346 herbicides and 68 ChI. Closer points on the plot denote more structurally similar compounds (Fig. 3a). Herbicides of the same class tend to cluster

as they share similar structural fragments [6]. Therefore, based on structural similarities, some of the ChI are grouped with some herbicides. More precisely, OP ChI (PChI, grey dots) are divided into two groups and five OP herbicides belonging to HRAC classes K1, K3 and N (Fig. 2) are positioned together with the PChI cluster in the lower right part of the t-SNE plot. Two herbicide carbamates, phenmedipham and desmedipham (C1), are arranged within the cluster of PChI and other ChI (black dots) in the central part of the t-SNE plot, which was expected as carbamates are known as potent ChE inhibitors [52]. On the other hand, terbutylazine (C1), tembotrione (F2), flufenacet (K3) and oxadiazon (E) are clustered with structurally similar herbicides apart from ChI clusters.

The PCA plot in Fig. 3b relates the physicochemical characteristics of the selected herbicides to those of ChI. Interestingly, ChI are scattered across the PCA plot due to their differences in logP, TPSA, and HBA values, which indicate their different physicochemical and ADME profiles. The most exposed outliers among ChI on the PCA plot were bis(18) huperzine B, acotiamide, demacarium, ambenonium chloride, and edrophonium. Compounds without CNS activity potential are positioned in the lower left quadrant. These ChI are predicted not to cross the BBB because of their unfavourable size, polarity, and relatively numerous atoms able to form hydrogen bonds. In general, all 11 selected herbicides, except glyphosate and tembotrione, fall within ranges of the physicochemical parameters relevant to CNS activity *i.e.* estimated to have potential for passive diffusion into the brain and achieving a relevant concentration for a physiological effect.

In general, commercial herbicides are small molecules with no more than two H-bond donor (HBD) atoms and a lipophilicity coefficient

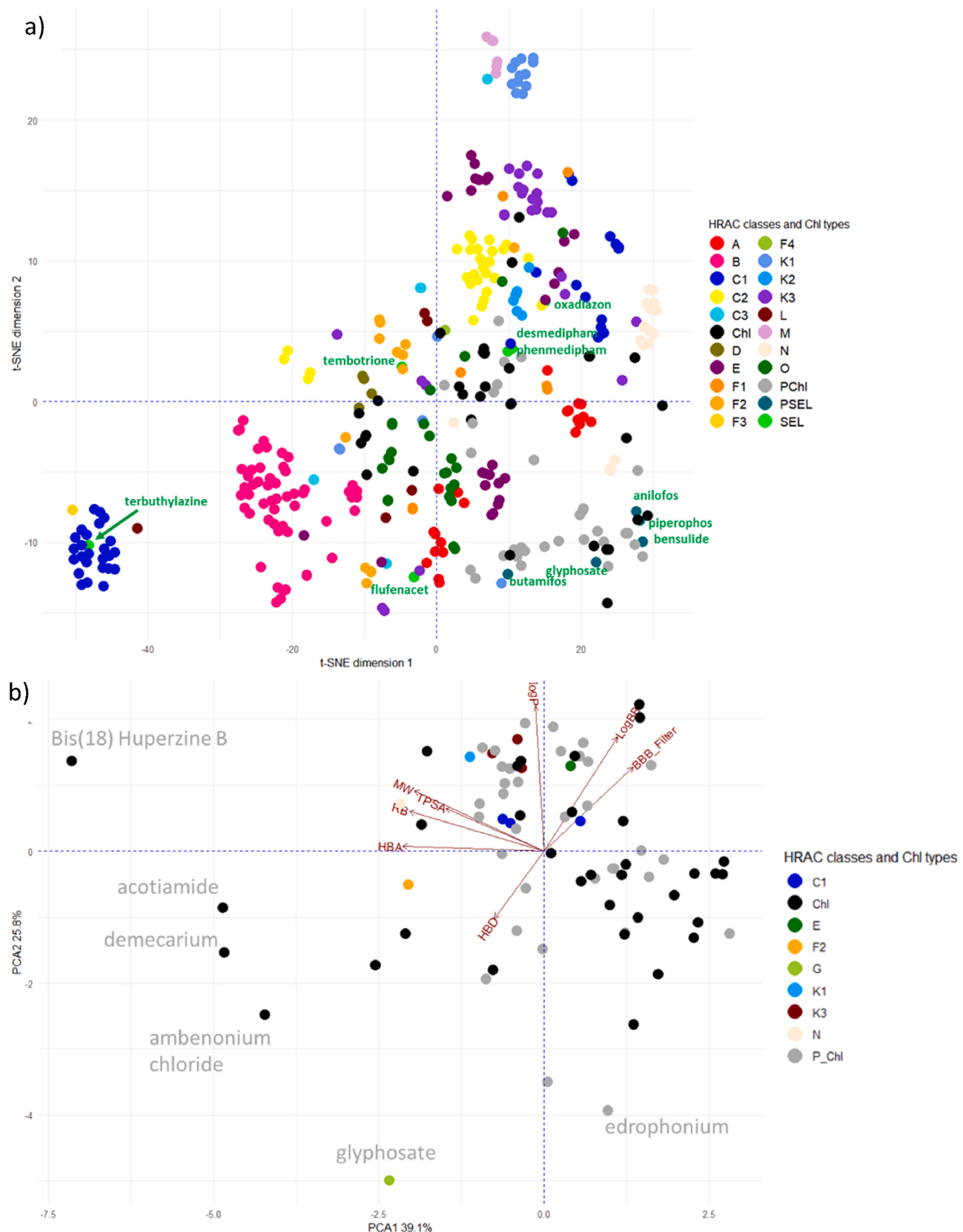


Fig. 3. a) t-SNE plot representing the grouping of 346 herbicides and 68 cholinesterase inhibitors (ChI) according to their structural similarity. Closer points denote more structurally similar compounds. SEL represents the selected herbicides, while PSEL and PChI represent the organophosphorus compounds from each category. Other herbicides are coloured and marked according to their legacy HRAC classes. b) PCA biplot representing distribution of 11 selected herbicides and 68 known ChI with regard to the physicochemical molecular features relevant for CNS activity (represented by red arrows; longer arrow means more important parameter for variance explanation within the analysed group of compounds). ChI denotes structurally diverse cholinesterase inhibitors, P_ChI are OP inhibitors, and the selected herbicides are coloured according to their legacy HRAC class.

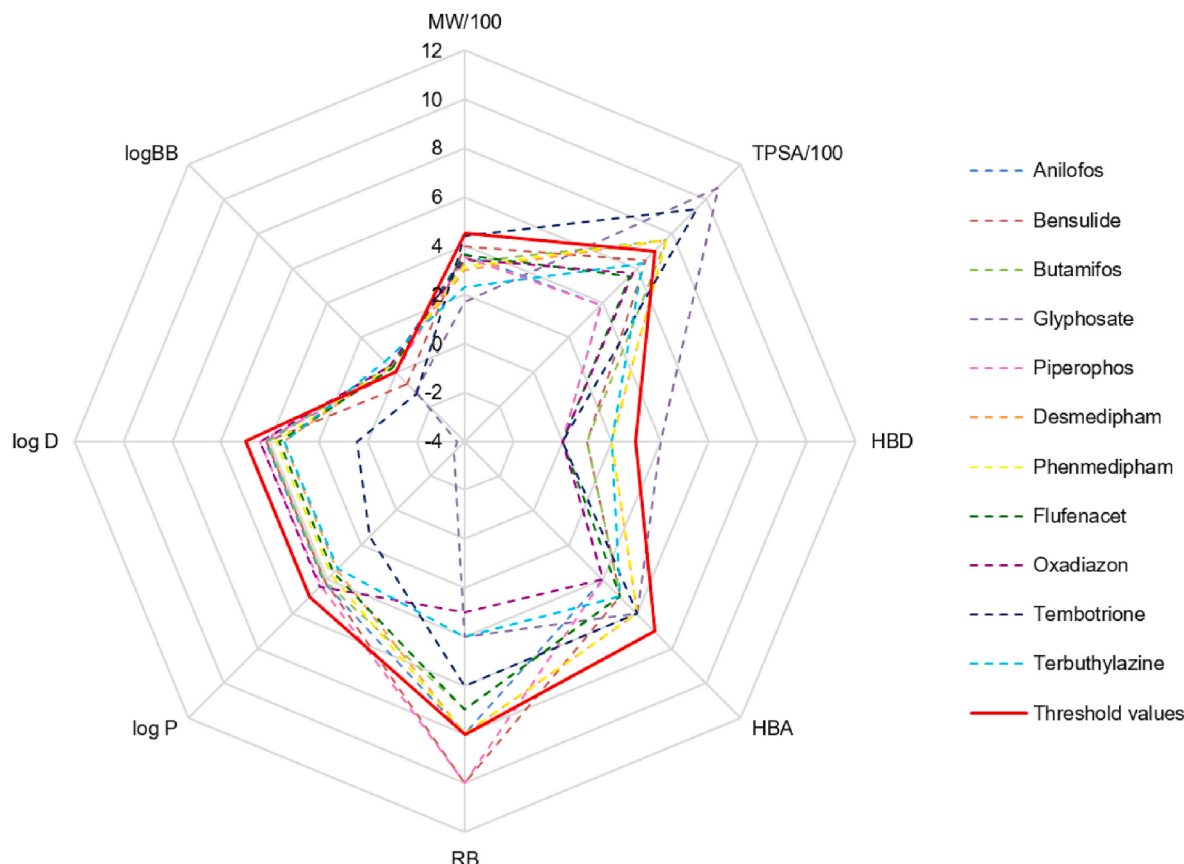


Fig. 4. Radar plot of physicochemical properties of 11 herbicides selected for *in vitro* testing (molecular weight, MW; topological polar surface area, TPSA; hydrogen bond donor, HBD; hydrogen bond acceptor, HBA; rotatable bonds, RB; lipophilicity coefficient, log P; distribution coefficient, log D; blood-brain barrier penetration, BBB; blood-brain barrier retention, logBB (Table S2). Upper recommended threshold values for molecular properties relevant for CNS activity are presented by a red line [36]. For logBB, acceptable values should be positioned outside the threshold line.

(logP) within the range 0.5–4.5 [6]. The analysis of physicochemical parameters for 11 selected herbicides depicted as a radar plot in Fig. 4 and as the PCA plot in Fig. 3b shows that glyphosate exceeds most of the cut-off values and is the most exposed outlier in the PCA plot. It is a polar molecule with a substantial number of HBD atoms and its physicochemical profile is unfavourable for CNS activity (Table S2). Besides glyphosate, only tembotrione has a TPSA value inappropriate for CNS activity. K3 class herbicides – anilofos, piperophos and flufenacet, possess favourable molecular properties for CNS activity. They are nonpolar and lipophilic molecules without HBD atoms and predicted to have considerable brain exposure. Accordingly, they are located in the upper part of the PCA plot along with other molecules, including 6 selected C1, E and K1 herbicides, with favourable properties for CNS activity (Fig. 3b).

Along with these analyses, glyphosate was selected as it is the most commonly used OP herbicide and, more importantly, there are controversial studies on its inhibitory activity towards AChE and BChE [53, 54]. A recent study with tembotrione at agronomical doses reported its inhibitory effect on the tyrosine pathway present in environmental bacterial strains as well as in a wide range of living organisms [55]. For terbutylazine and oxadiazon there is also no inhibitory data but neurotoxic effects have been well documented on oxadiazon [56], and atrazine, an analogue of terbutylazine [57,58], possibly leading to neurodegenerative conditions. It is worth mentioning that the selected herbicides were predicted to have toxic effects on *T. pyriformis* and *D. magna*, as model organisms for possible neuromodulating effects [17, 18].

Table 2

Inhibition of human AChE and BChE by eleven herbicides in terms of IC₅₀ value (\pm S.E.) determined from at least three experiments measured after 30 min of incubation at 25 °C.

Herbicide	IC ₅₀ /μM	
	AChE	BChE
Anilofos	25 ± 10	8.6 ± 0.7
Bensulide	120 ± 80	13 ± 5
Butamifos	≈100	15 ± 4
Glyphosate	>1,000	>1,000
Piperophos	>100	7.0 ± 0.8
Desmedipham	138 ± 85	26 ± 5
Phenmedipham	41 ± 18	30 ± 6
Flufenacet	48 ± 20	6.4 ± 0.8
Oxadiazon	≥ 100	≥ 100
Tembotrione	≥ 100	≥ 100
Terbutylazine	≥ 100	≥ 100

3.4. Evaluation of potency of cholinesterase inhibition by the selected herbicides

Activity of human AChE and BChE was measured in the presence of the selected herbicides (Fig. 2) to estimate the inhibition potency given in Table 2 and Fig. S3. Since we expected that some of the selected herbicides could act as a hemi-substrate of cholinesterases, i.e. progressively inhibit the enzymes, the enzyme activity was measured after 30 min of incubation. In other words, we ensured a valid comparison of inhibition potency in terms of IC₅₀ between the selected organophosphates, carbamates, oxyacetanilide, oxadiazolone, triketone and

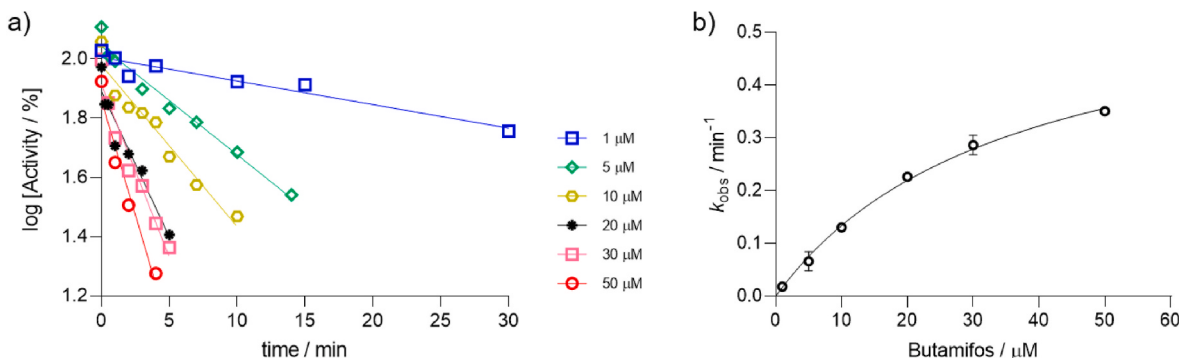


Fig. 5. Progressive inhibition of human plasma BChE with butamifos. a) Representative experiment for time-course inhibition of BChE with butamifos; the slope determines the observed first-order rate constant, k_{obs} . b) Constants k_{obs} were plotted as a function of butamifos concentration wherefrom kinetic parameters of BChE phosphorylation were determined: the first-order inhibition constant (k_{max}) was $0.61 \pm 0.06 \text{ min}^{-1}$, enzyme-inhibitor equilibrium dissociation constant (K_i) was $35 \pm 6 \mu\text{M}$ and the overall second-order rate constant of inhibition (k_i) was $17,200 \pm 1,500 \text{ min}^{-1}\text{M}^{-1}$.

triazine.

Anilofos, flufenacet and phenmedipham were potent inhibitors of both AChE and BChE, with the IC_{50} values in low micromolar range (6–50 μM). The carbamate desmedipham and four tested organophosphates, anilofos, bensulfide, butamifos and piperophos, were more potent inhibitors of BChE than AChE. Therefore, they could be considered selective BChE inhibitors, while the highest selectivity, at least 10-times, was observed with piperophos and butamifos as their AChE IC_{50} value were approximated to be higher than the highest tested concentration of 100 μM (Table 2, Fig. S3).

Glyphosate, oxadiazon, tembotriione and terbutylazine showed poor inhibitor potency for both AChE and BChE (Fig. S3). Inhibition of both enzymes with the highest concentration of these compounds was less than 10–20% and their IC_{50} values were only estimated to be above 100 μM , or above 1 mM in case of glyphosate. Our result on glyphosate is in agreement with a study on human erythrocyte AChE and its 10% and 20% of inhibition with 0.1 and 5.0 mM glyphosate, respectively [54]. Additionally, its weak potency to inhibit BChE agrees with the finding of a recent study that, considering that it did not inhibit BChE at a concentration of 1 mM, glyphosate showed specificity for AChE but low inhibitory capacity [59].

Nevertheless, organophosphates and carbamates belonging to HRAC classes C1, K1, N, and K3 were confirmed as potent inhibitors of human cholinesterases, supporting our t-SNE analysis and prediction. Interesting to note is that K3 class herbicides, flufenacet and anilofos, the most potent inhibitors of both cholinesterases, share a N-(4-halophenyl)-N-propan-2-yl acetamide fragment. Also, as they were predicted to have good potential of crossing the BBB and being active in the CNS, they both pose a danger in cases of acute or chronic poisoning. However, our *in vitro* assays showed that all of the selected herbicides were more potent inhibitors of BChE, which is a valuable indication of their metabolic degradation by plasma BChE before the herbicide reaches the CNS [25].

3.5. Time-dependent inhibition of AChE and BChE by the selected herbicides

We examined the time-course of ChE inhibition by anilofos, bensulfide, butamifos and piperophos. Inhibition of BChE with butamifos displayed progressive inhibition (Fig. 5). Due to the accumulation of the Michaelis-type complex, a saturation curve was observed, which enabled the determination of the overall second-order constant of phosphorylation (k_i), the first-order inhibition constant (k_{max}) and enzyme-inhibitor equilibrium dissociation constant (K_i) [41]. Its overall inhibition constant ($k_i = 17,170 \pm 1,522 \text{ min}^{-1}\text{M}^{-1}$) sorted phosphorothioate butamifos with oxono-phosphate insecticides that inhibited BChE with similar rates [60]. Such high potency was not expected, since phosphorothioates are usually less toxic and potent inhibitors than

phosphate pesticides with a P=O bond [61]. An additional comparison with the rates reported for structurally similar fenamiphos shows that butamifos due to its lower affinity is not an even more potent inhibitor of BChE, although its first-order inhibition constant ($k_{max} = 0.61 \pm 0.06 \text{ min}^{-1}$) is almost 4-times faster than that of fenamiphos [60].

The time-course inhibition of AChE and BChE by other OP herbicides, given in Fig. S4, is a somewhat different course of inhibition than observed with BChE and butamifos. After initial (and short) first-order kinetics, inhibition of AChE and BChE with anilofos reached an equilibrium, while inhibition with other herbicides can be approximated to slower first-order kinetics. In other words, with the highest tested herbicide concentration the activity decreased to below 5%. Based on other studies, a possible interpretation of these curves is a fast spontaneous reactivation and possible aging reaction as was reported on trialkyl phosphorothiolates [20,62].

Furthermore, all OP herbicides generated a considerable amount of reversible complex given with y-axis intercepts, meaning that both progressive and reversible inhibition is a consequence of simultaneous covalent and non-covalent enzyme-inhibitor interactions [41]. Additional experiments are needed for a mechanistic evaluation of cholinesterases inhibition with herbicides. It is worth mentioning that Reiner and Aldridge [20] proposed that in addition to progressive phosphorylation of active site, binding of compounds to the peripheral site produced reversible inhibition, which decreased substrate hydrolysis in a manner similar to the phenomenon of AChE allosteric substrate inhibition.

3.6. Molecular modelling of AChE and BChE interactions with selected herbicides

Molecular modelling of Michaelis-type complex of selected herbicides within the active sites of two human cholinesterases enabled us to identify interactions between herbicide molecules and amino acid residues lining the active site gorge. In case of organophosphates and carbamates, the main criteria for selection of binding position of herbicide within the AChE or BChE catalytic sites was the orientation of the leaving group of the herbicide oriented opposite from the oxygen (O_y) of the enzyme catalytic serine mimicking orientation productive for the nucleophilic attack by the catalytic serine during enzyme progressive inhibition by acylating agents such as organophosphates and carbamates. Generally, ChE can be described as ligands having aromatic groups e.g. quinolines or benzopyrans that create cation- π and/or π - π interactions with Trp86 and Trp286, key residues of the CBS (choline binding site) and PAS (peripheral anionic site). Ligands long enough to bind simultaneously in the CBS and the PAS are more potent inhibitors of AChE, e.g. donepezil. HBD or HBA atoms present in the ligand also contribute to potency of inhibition [63]. The list of non-bond

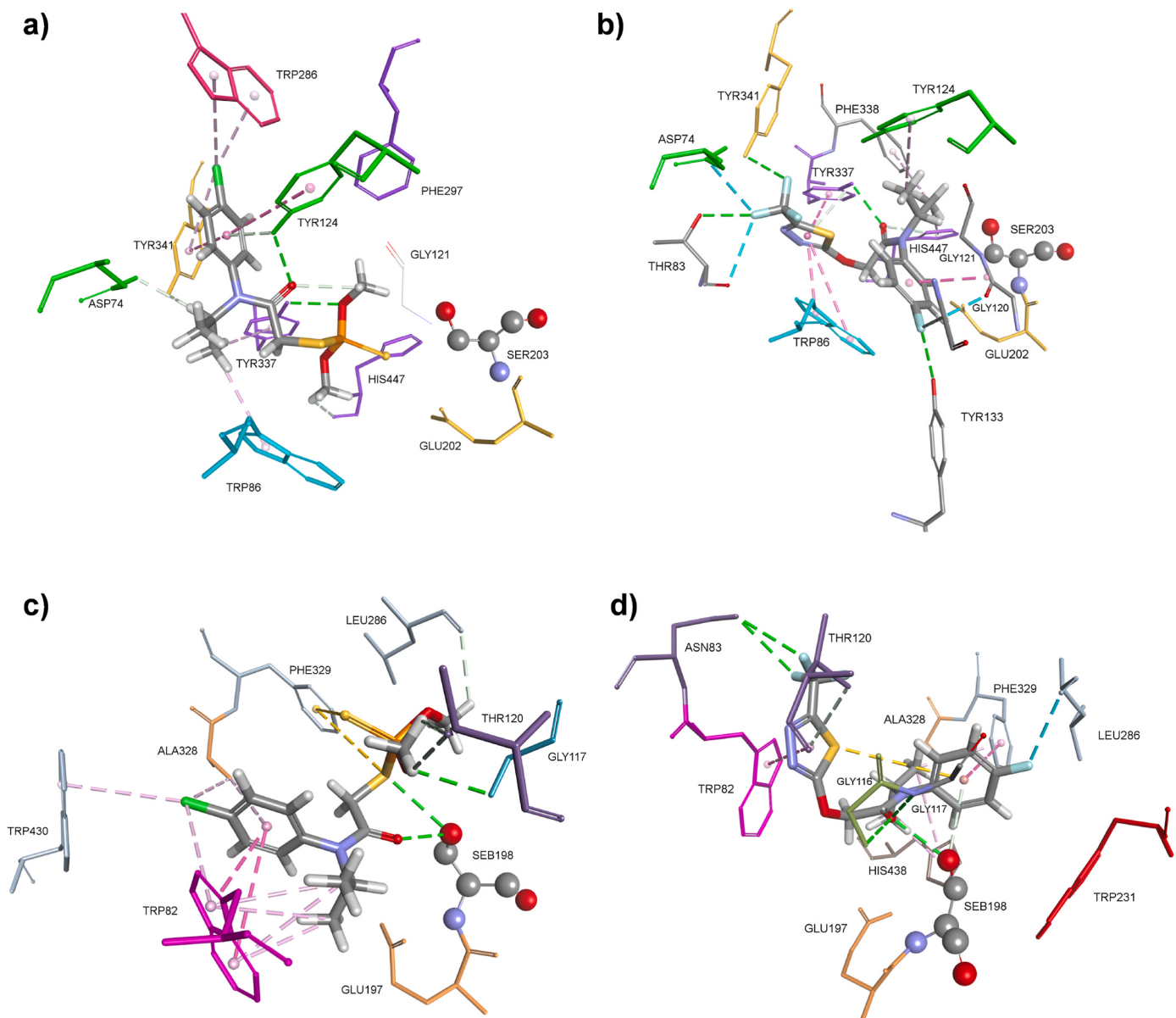


Fig. 6. Model of Michaelis-type complex of herbicides: anilofos (a) and flufenacet (b) within the active site of human AChE (PDB code: 4PQE) [44], and anilofos (c) and flufenacet (d) within the active site of human BChE (PDB code: 2PM8) [45]. Poses were selected based on criteria that the leaving group of herbicide is oriented opposite from the oxygen (O_γ) of catalytic serine (AChE - Ser203, BChE - Ser198). Interactions are represented as dashed lines: hydrophobic (purple), hydrogen bonds (green) and electrostatic (orange).

interactions formed between selected herbicides and AChE and BChE is given in Table S4.

Fig. 6 shows docking results for the most potent inhibitors of AChE and BChE, anilofos and flufenacet. Although they share a common feature of having a tertiary amine with the neighbouring carbonyl, isopropyl and halogenated phenyl group, including a chlorine or fluorine atom, their interactions with AChE active site residues differ. Anilofos is stabilized by hydrophobic interactions with Trp86 and Tyr 337 from the CBS and Tyr124 and Trp286 from the PAS (Fig. 6a). Additional stabilization is also provided because the chlorophenyl group is well positioned between Tyr341 and the mentioned Tyr124 and Trp286 from the PAS. It can be seen that catalytic Ser203 can perform the nucleophilic attack toward the electrophilic phosphorus atom of anilofos. Positioning of flufenacet shows a different orientation of the isopropyl group, away from Trp86, forming hydrophobic interactions with Tyr124 and Phe338 (Fig. 6b). Additionally, trifluoromethyl thiadiazol ring is positioned in the CBS, forming hydrophobic interactions with Trp86 and

Tyr337 and hydrogen bonds with Asp74, Thr83 and Tyr341. Compared to anilofos, a lower position of flufenacet in the AChE active site causes a lack of interaction with the Trp286 from the PAS.

Molecular modelling of the herbicide-BChE complex revealed interactions with residues that stabilise anilofos in a favourable position to covalently inhibit catalytic serine, while the leaving group is in an opposite direction from Ser198. Both anilofos and flufenacet are positioned close to the catalytic Ser198 forming a hydrogen bond with it (Fig. 6c and d), primarily due to the difference between BChE and AChE active site gorges. Anilofos creates multiple hydrophobic interactions with Trp82 from CBS with its chlorophenyl group and isopropyl group (Fig. 6c). The chlorophenyl group is additionally stabilized with Ala328 and Trp430. Flufenacet's fluorophenyl group is positioned in the acyl pocket and stabilized via a hydrogen bond with Leu286 and hydrophobic bond with Phe329 (Fig. 6d). It creates an additional hydrogen bond with Ser198. The amide oxygen from flufenacet is stabilized in the oxyanion hole creating hydrogen bonds with the same amino acid

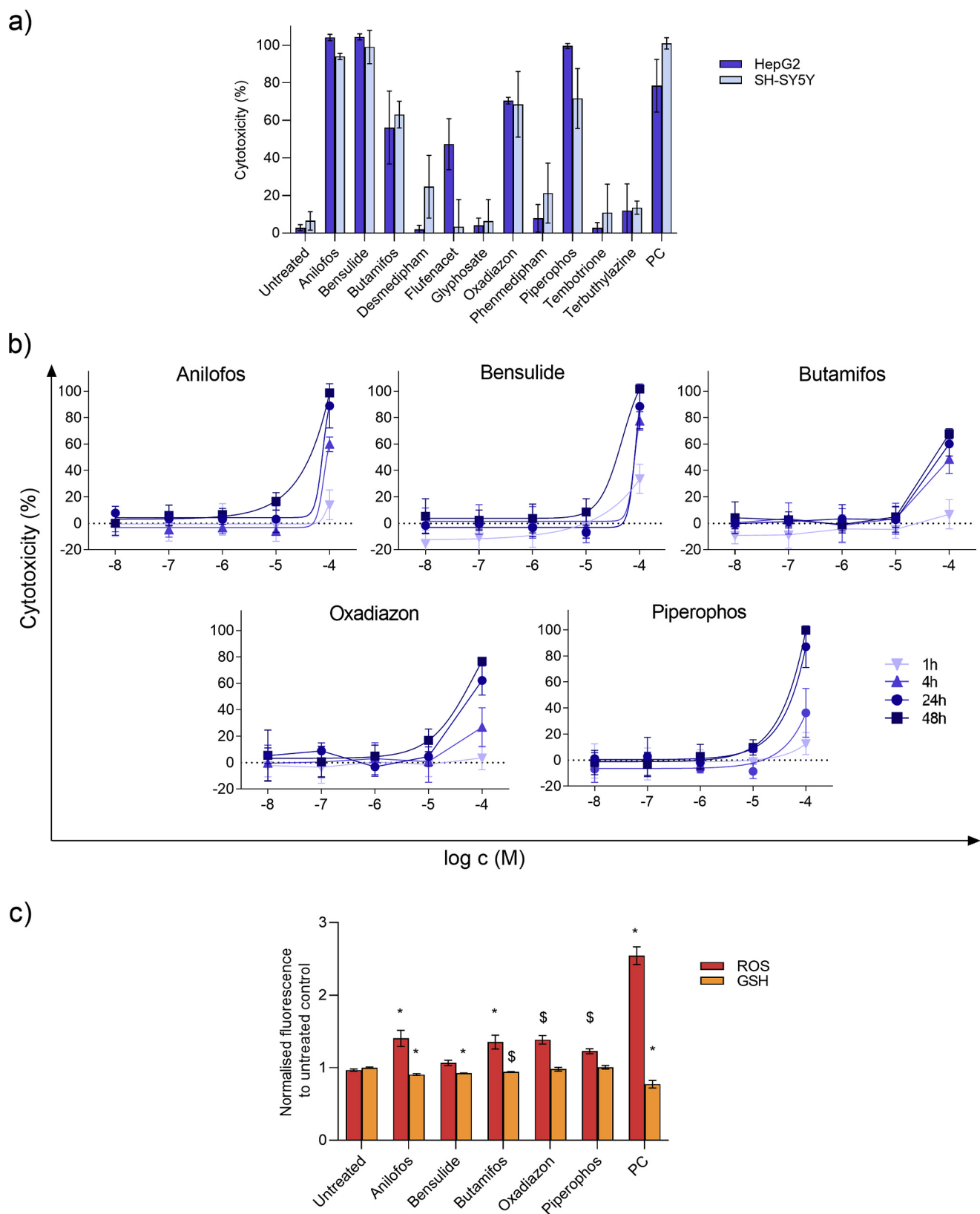


Fig. 7. Cytotoxicity of selected herbicides and oxidative status of cells. a) Cytotoxicity evaluated on HepG2 and SH-SY5Y cell lines by MTS assay after 24 h exposure to herbicides (100 μ M); stauroporine (3 μ M) was used as a positive control (PC). b) Concentration- and time-dependent cytotoxicity of herbicides evaluated on SH-SY5Y cells after 1, 4, 24 and 48 h exposure. c) Fluorescence indicating ROS or GSH levels evaluated on SH-SY5Y cells after 1 h exposure. PCs were: H₂O₂ (100 μ M) for ROS induction and tBOOH (100 μ M) for GSH consumption experiments. Statistical significance: Ordinary one-way ANOVA – Dunnett's test (#p < 0.01; \$p < 0.01; *p < 0.0001).

residues as the carbamates, while its trifluoromethyl thiadiazole group is positioned in CBS creating a hydrophobic interaction with Trp82 and hydrogen bonds with Asn83 and Thr120. Docking results for complexes between other herbicides in this study and AChE and BChE are given in Fig. S5 and Fig. S6, respectively. Nevertheless, on the basis of the set of interactions between the herbicides and residues within the gorge, it can be hypothesized that the studied compounds could act as “bulky”-blockers of substrate binding at the catalytic site.

3.7. Cytotoxicity and oxidative status of selected herbicides

Cytotoxicity of selected herbicides was evaluated on neural SH-SY5Y and liver HepG2 cells after a 24 h exposure period. For the screening, we chose 100 μ M concentration of herbicides. Out of the 11 tested herbicides, four phosphorothioates (anilofos, bensulide, butamifos, piperophos) and oxadiazon showed high cytotoxic effects on both cell lines, and flufenacet on HepG2 (Fig. 7a). It is worth emphasizing that in our experiments glyphosate, tembotrione, terbutylazine, desmedipham, and phenmedipham did not exhibit significant toxicity.

Furthermore, cytotoxic herbicides were tested in a concentration- and time-dependant manner on HepG2 cells as a model. Since HepG2 cells exhibit high metabolic activity, the observed toxic effect might be due to the formed herbicide metabolites. Therefore, the observed time-dependent effect on cells could also refer to a scenario recently reported for flufenacet [64]. As the results showed, the selected herbicides were not cytotoxic up to a 10 μ M concentration at any of the time points tested (Fig. 7b). However, at 100 μ M, a cytotoxic effect was observed already after 1 h of exposure indicating a fast process of cell death caused likely by the original compound itself.

To investigate if the disrupted oxidative/antioxidative chain could have been a trigger for the observed fast cytotoxicity, induction of reactive oxygen species (ROS) and glutathione (GSH) consumption were measured 1 h after exposure to herbicides (100 μ M) on SH-SY5Y cells as a model. As the results presented in Fig. 7c indicate, all of the tested herbicides increased levels of ROS except bensulide. However, bensulide as well as anilofos and butamifos reduced the intracellular GSH level. The induction of ROS and/or decreased GSH levels indicated a deterioration of the antioxidant system and the development of oxidative stress, which can lead to cell death and development of diseases [65].

It is worth commenting that the K3 (anilofos and piperophos) and N class (bensulide) of herbicides were cytotoxic to neural and hepatic cells, but at a high concentration, probably not sufficiently enough to be present in the body even in the case of their accumulation [10]. Depending on the structure of the selected herbicides, phosphorothioates were the most toxic ones and this was also predicted by *in silico* analysis. Surprisingly, no time-dependence of the cytotoxic effect was observed, which may suggest that cell death was generated by the activation of an unregulated membrane burst via lactate dehydrogenase associated with cell stress [51,66]. In other words, the cytotoxicity observed here was not a direct consequence of AChE inhibition but rather a result of some other mechanism. However, possible cytotoxic effects *in vivo* connected to the inhibition are likely to be present during neurodevelopment, as both AChE and BChE have a “morphogenic” role in vertebrate systems linked to the spatiotemporal acetylcholine hydrolysis during brain development [67,68].

Nevertheless, the non-cytotoxicity of tested herbicides does not exclude their primary mechanism of action and possible toxicity upon chronic/multiple exposure *in vivo*. So for example, it was shown that piperophos caused a significant decrease in testosterone biosynthesis by Leydig cells that pose a serious threat to the male reproductive system [69], while oxadiazon demonstrated potential for reproductive toxicity and endocrine disruptor activity [70]. In case of glyphosate and its metabolite aminomethylphosphonic acid, it has been well documented that they induce pronounced cytotoxicity and neurotoxicity in SH-SY5Y cells through increasing ROS and by altering the expression of genes related to neuronal development, apoptosis and autophagy [71].

Moreover, the IC₅₀ value was calculated to be 5.36 \pm 1.12 mM for glyphosate on SH-SY5Y cells [71]. Our results on carbamates phenmedipham and desmedipham were in accordance with the EFSA and available data which did not raise concern in relation to neurotoxicity or immunotoxicity [72,73]. However, we should also mention the possible toxic effects of commercial preparations of herbicide mixtures. Indeed, desmedipham and phenmedipham in a commercial mixture with ethofumesate (N/K3) showed reproductive and developmental toxicity on *Daphnia* spp [15].

4. Conclusion

The comprehensive computational analysis of 346 commercially available herbicides and additional 163 herbicides no longer in use firmly points towards their prevailing potential for reproductive/developmental toxicity and neurotoxicity. The chemical structure of herbicides governs not only their modes of action but also their toxicity. For each herbicide class there is at least one warning of possible toxicity, while the classes with multiple alerts are K1, K3, M, F1 and E (legacy HRAC classification) and additional A and K2 classes specifically for 163 outdated herbicides. Generally, comparison of these two sets of herbicides revealed similar physicochemical profiles from respective classes, but commercial herbicides were significantly less toxic concerning chromosomal aberrations and bioaccumulation. Our study on human cholinesterases describes the binding potency, inhibition and selectivity of the selected herbicides. It is worth pointing out that organophosphate herbicides - anilofos, bensulide and piperophos inhibit both cholinesterases through a network of non-covalent and covalent interactions, while butamifos inhibits only through covalent binding to the catalytic serine. These findings along with the observed cytotoxicity on neuronal and hepatic cells give insight into the potential toxic effects of herbicides in use and can be used in the development of novel herbicides with less deleterious effects to humans and the environment.

Author contributions

Conceptualization, V.S. and Z.K.; experimental analysis, V.P., D.K., A.Z., G.Š., and V.S.; funding acquisition, M.K. and Z.K.; supervision, V.S. and Z.K.; writing—original draft, V.P. and D.K.; writing—review and editing V.P., D.K., A.Z., G.Š., M.K., V.S. and Z.K. All authors have read and agreed to the published version of the manuscript.

Declaration of competing interest

The authors declare that they have no known competing financial interests or personal relationships that could have appeared to influence the work reported in this paper.

Data availability

Data will be made available on request.

Acknowledgement

The authors are grateful to Dr Xavier Brazzolotto and Dr Florian Nathon for AChE and BChE, and Dr Davor Želježić and Dr Vilena Kašuba for glyphosate, tembotrione, and terbutylazine. V.S. would like to acknowledge the use of the program ADMET Predictor acquired by the project Bioprospecting of the Adriatic Sea (KK.01.1.1.01.0002). This work was supported by the Croatian Science Foundation (IP-2018-01-7683 and UIP-2017-05-7260).

Appendix A. Supplementary data

Supplementary data to this article can be found online at <https://doi.org/10.1016/j.cbi.2023.110506>. Contents: 1. *In silico* toxicity profiling

of herbicides no longer in use, 2. Physicochemical parameters relevant for CNS activity estimated for herbicides no longer in use; 3. Toxicity parameters of the selected herbicides, 4. IC₅₀ curves of human AChE and BChE in presence of selected herbicides, 5. Time-course inhibition of human AChE and BChE by organophosphate herbicides, and 6. Molecular modelling of complexes between herbicides and cholinesterases.

References

- [1] C. Bolognesi, F.D. Merlo, Pesticides: human health effects, in: Encyclopedia of Environmental Health, Elsevier, 2011, pp. 438–453.
- [2] V.I. Lushchak, T.M. Matviishyn, V. Husak, J.M. Storey, K.B. Storey, Pesticide toxicity: a mechanistic approach, EXCLI J 17 (2018) 1101–1136.
- [3] A. Forouzesh, E. Zand, S. Soufizadeh, S. Samadi Foroushani, Classification of herbicides according to chemical family for weed resistance management strategies - an update, Weed Res. 55 (4) (2015) 334–358.
- [4] S.I. Sherwani, I.A. Arif, H.A. Khan, Modes of action of different classes of herbicides, in: Herbicides, Physiology of Action, and Safety, InTech, 2015.
- [5] S.O. Duke, Overview of herbicide mechanisms of action, Environ. Health Perspect. 87 (1990) 263–271.
- [6] D. Oršolić, V. Pehar, T. Šmuc, V. Stepanić, Comprehensive machine learning based study of the chemical space of herbicides, Sci. Rep. 11 (1) (2021), 11479.
- [7] Herbicide resistance action committee (HRAC), Available from: <https://www.hracglobal.com/>.
- [8] FAO, Pesticides Use, Pesticides Trade and Pesticides Indicators - Global, Regional and Country Trends, 1990–2020, vol. 46, FAOSTAT Analytical Briefs, Rome, 2022.
- [9] H.R. Köhler, R. Triebeskorn, Wildlife ecotoxicology of pesticides: can we track effects to the population level and beyond? Science 341 (6147) (2013) 759–765.
- [10] V.P. Kalyabina, E.N. Esimbekova, K.V. Kopylova, V.A. Kratasyuk, Pesticides: formulants, distribution pathways and effects on human health – a review, Toxicol Rep 8 (2021) 1179–1192.
- [11] J.R. Richardson, V. Fitsanakis, R.H.S. Westerink, A.G. Kanthasamy, Neurotoxicity of pesticides, Acta Neuropathol. 138 (3) (2019) 343–362.
- [12] S. Mostafalou, M. Abdollahi, Pesticides: an update of human exposure and toxicity, Arch. Toxicol. 91 (2) (2017) 549–599.
- [13] R. Maurya, A.K. Pandey, Importance of protozoa *Tetrahymena* in toxicological studies: a review, Sci. Total Environ. 741 (2020), 140058.
- [14] J.L. Bonnet, F. Bonnemoy, M. Dusser, J. Bohatier, Assessment of the potential toxicity of herbicides and their degradation products to nontarget cells using two microorganisms, the bacteria *Vibrio fischeri* and the ciliate *Tetrahymena pyriformis*, Environ. Toxicol. 22 (1) (2007) 78–91.
- [15] T. Vidal, J.L. Pereira, N. Abrantes, A.M.V.M. Soares, F. Gonçalves, Reproductive and developmental toxicity of the herbicide Betanal® Expert and corresponding active ingredients to *Daphnia* spp, Environ. Sci. Pollut. Res. Int. 23 (13) (2016) 13276–13287.
- [16] F. Corotto, D. Ceballos, A. Lee, L. Vinson, Making the most of the daphnia heart rate lab: optimizing the use of ethanol, nicotine & caffeine, Am. Biol. Teach. 72 (3) (2010) 176–179.
- [17] M. Bellot, M. Faria, C. Gómez-Canela, D. Raldúa, C. Barata, Pharmacological modulation of behaviour, serotonin and dopamine levels in *Daphnia magna* exposed to the monoamine oxidase inhibitor deprenyl, Toxics 9 (8) (2021) 187.
- [18] A. Tziakouri, E. Lajkó, L. Kohidai, The phylogenetic background of neurotransmitters in the unicellular organism *Tetrahymena pyriformis*, Ann Behav Neurosci 1 (2018) 108–118.
- [19] A. Ud-Daula, G. Pfister, K.W. Schramm, Growth inhibition and biodegradation of catecholamines in the ciliated protozoan *Tetrahymena pyriformis*, J Environ Sci Health A Tox Hazard Subst Environ Eng 43 (14) (2008) 1610–1617.
- [20] W.N. Aldridge, E. Reiner, Enzyme Inhibitors as Substrates. Interactions of Esterases with Esters of Organophosphorus and Carbamic Acids, North-Holland Pub. Co, Amsterdam, 1972.
- [21] A. Chatonet, O. Lockridge, Comparison of butyrylcholinesterase and acetylcholinesterase, Biochem. J. 260 (3) (1989) 625–634.
- [22] T. Zorbaz, Z. Kovarik, Neuropharmacology: oxime antidotes for organophosphate pesticide and nerve agent poisoning, Period. Biol. 121–122 (1–2) (2020) 35–54.
- [23] C.M. Timperley, M. Abdollahi, A.S. Al-Amri, A. Baulig, D. Benachour, V. Borrett, et al., Advice on assistance and protection by the Scientific Advisory Board of the Organisation for the Prohibition of Chemical Weapons: Part 2. On preventing and treating health effects from acute, prolonged, and repeated nerve agent exposure, and the identification of medical countermeasures able to reduce or eliminate the longer term health effects of nerve agents, Toxicology 413 (2019) 13–23.
- [24] Y. Yurumez, P. Durukan, Y. Yavuz, I. Ikitzeli, L. Avsarogullari, S. Ozkan, et al., Acute organophosphate poisoning in university hospital emergency room patients, Intern. Med. 46 (13) (2007) 965–969.
- [25] P. Masson, F. Nachon, Cholinesterase reactivators and bioscavengers for pre- and post-exposure treatments of organophosphorus poisoning, J. Neurochem. 142 (Suppl 2) (2017) 26–40.
- [26] T. Čadež, Z. Kovarik, Advancements in recombinant technology for production of butyrylcholinesterase, a bioscavenger of nerve agent, Period. Biol. 121–122 (1–2) (2020) 55–63.
- [27] N. Macek Hrvat, Z. Kovarik, Counteracting poisoning with chemical warfare nerve agents, Arh. Hig. Rada. Toksilok. 71 (4) (2020) 266–284.
- [28] Compendium of pesticide common Names, Available from: <http://www.bcppesticidecompendium.org/>.
- [29] Pesticide properties DataBase (PPDB), Available from: <http://sitem.herts.ac.uk/aeru/ppdb/>.
- [30] S. Kim, J. Chen, T. Cheng, A. Gindulyte, J. He, S. He, et al., PubChem 2023 update, Nucleic Acids Res. 51 (D1) (2023) D1373–D1380.
- [31] J. Gong, X. Liu, X. Cao, Y. Diao, D. Gao, H. Li, et al., PTID: an integrated web resource and computational tool for agrochemical discovery, Bioinformatics 29 (2) (2013) 292–294.
- [32] A. Gaulton, A. Hersey, M. Nowotka, A.P. Bento, J. Chambers, D. Mendez, et al., The ChEMBL database in 2017, Nucleic Acids Res. 45 (D1) (2017) D945–D954.
- [33] ADMET Predictor. <https://www.simulations-plus.com/software/admetpredictor/>.
- [34] T. Sander, J. Freyss, M. von Korff, C. Rufener, DataWarrior: an open-source program for chemistry aware data visualization and analysis, J. Chem. Inf. Model. 55 (2) (2015) 460–473.
- [35] D. Rogers, M. Hahn, Extended-connectivity fingerprints, J. Chem. Inf. Model. 50 (5) (2010) 742–754.
- [36] H. Pajouhesh, G.R. Lenz, Medicinal chemical properties of successful central nervous system drugs, NeuroRx 2 (4) (2005) 541–553.
- [37] RStudio. <http://www.rstudio.com/>.
- [38] G.L. Ellman, K.D. Courtney, V. Andres, R.M. Featherstone, A new and rapid colorimetric determination of acetylcholinesterase activity, Biochem. Pharmacol. 7 (2) (1961) 88–95.
- [39] Z. Kovarik, A. Bosak, G. Šinko, T. Latas, Exploring the active sites of cholinesterases by inhibition with bambuterol and haloxon, Croat. Chem. Acta 76 (1) (2003) 63–67.
- [40] Motulsky H.J. GraphPad prism 8 curve fitting guide - equation: two phase decay. GraphPad Prism 9.
- [41] Z. Kovarik, Z. Radić, H.A. Berman, V. Simeon-Rudolf, E. Reiner, P. Taylor, Acetylcholinesterase active centre and gorge conformations analysed by combinatorial mutations and enantiomeric phosphonates, Biochem. J. 373 (1) (2003) 33–40.
- [42] F.A. Momany, R. Rone, Validation of the general purpose QUANTA ®3.2/CHARMM® force field, J. Comput. Chem. 13 (7) (1992) 888–900.
- [43] B.R. Brooks, R.E. Bruccoleri, B.D. Olafson, D.J. States, S. Swaminathan, M. Karplus, CHARMM: a program for macromolecular energy, minimization, and dynamics calculations, J. Comput. Chem. 4 (2) (1983) 187–217.
- [44] O. Dym, T. Unger, L. Toker, I. Silman, J.L. Sussman, Israel Structural Proteomics Center (ISPC). Crystal Structure of Human Acetylcholinesterase, 2015. Available from: https://www.wwpdb.org/pdb?id=pdb_00004pge.
- [45] M.N. Ngamelue, K. Homma, O. Lockridge, O.A. Asojo, Crystallization and X-ray structure of full-length recombinant human butyrylcholinesterase, Acta Crystallogr. 10 (9) (2007) 723–727, 63.
- [46] N. Maraković, A. Knežević, V. Vinković, Z. Kovarik, G. Šinko, Design and synthesis of N-substituted-2-hydroxyiminoacetamides and interactions with cholinesterases, Chem. Biol. Interact. 259 (2016) 122–132.
- [47] N. Maraković, A. Knežević, I. Rončević, X. Brazzolotto, Z. Kovarik, G. Šinko, Enantioseparation, in vitro testing, and structural characterization of triple-binding reactivators of organophosphate-inhibited cholinesterases, Biochem. J. 477 (15) (2020) 2771–2790.
- [48] E.C.A.C.C. Handbook, Fundamental Techniques in Cell Culture Laboratory Handbook, fourth ed., Merck KGaA, Darmstadt, Germany, 2018. Available from: <https://www.sigmapaldrich.com/life-science/cell-culture/learning-center/ecacc-h-andbook.html>.
- [49] R. Dulbecco, M. Vogt, Plaque formation and isolation of pure lines with poliomyelitis viruses, J. Exp. Med. 99 (2) (1954) 167–182.
- [50] T. Mosmann, Rapid colorimetric assay for cellular growth and survival: application to proliferation and cytotoxicity assays, J. Immunol. Methods 65 (1–2) (1983) 55–63.
- [51] A. Zandonà, N. Maraković, P. Mišetić, J. Madunić, K. Miš, J. Padovan, et al., Activation of (un)regulated cell death as a new perspective for bispyridinium and imidazolium oximes, Arch. Toxicol. 95 (8) (2021) 2737–2754.
- [52] A. Matosović, A. Bosak, Carbamate group as structural motif in drugs: a review of carbamate derivatives used as therapeutic agents, Arh. Hig. Rada. Toksilok. 71 (4) (2020) 285–299.
- [53] M. Milić, S. Žunec, V. Micek, V. Kašuba, A. Mikolić, B.T. Lovaković, et al., Oxidative stress, cholinesterase activity, and DNA damage in the liver, whole blood, and plasma of Wistar rats following a 28-day exposure to glyphosate, Arh. Hig. Rada. Toksilok. 69 (2) (2018) 154–168.
- [54] M. Kwiatkowska, H. Nowacka-Krukowski, B. Bukiowska, The effect of glyphosate, its metabolites and impurities on erythrocyte acetylcholinesterase activity, Environ. Toxicol. Pharmacol. 37 (3) (2014) 1101–1108.
- [55] C. Thiori-Mauprivez, F.E. Dayan, H. Terol, M. Devers, C. Calvayrac, F. Martin-Laurent, et al., Assessing the effects of β-triketone herbicides on HPPD from environmental bacteria using a combination of *in silico* and microbiological approaches, Environ. Sci. Pollut. Res. Int. 30 (4) (2022) 9932–9944.
- [56] D. Degl'Innocenti, M. Ramazzotti, E. Sarchielli, D. Monti, M. Chevanne, G. B. Vannelli, et al., Oxadiazon affects the expression and activity of aldehyde dehydrogenase and acylphosphatase in human striatal precursor cells: a possible role in neurotoxicity, Toxicology 411 (2019) 110–121.
- [57] K. Ma, H.Y. Wu, B. Zhang, X. He, B.X. Li, Neurotoxicity effects of atrazine-induced SH-SY5Y human dopaminergic neuroblastoma cells via microglial activation, Mol. Biosyst. 11 (11) (2015) 2915–2924.
- [58] C. Martins-Gomes, T.L. Silva, T. Andreani, A.M. Silva, Glyphosate vs. glyphosate-based herbicides exposure: a review on their toxicity, J. Xenobiot 12 (1) (2022) 21–40.

- [59] C. Martins-Gomes, T.E. Coutinho, T.L. Silva, T. Andreani, A.M. Silva, Neurotoxicity assessment of four different pesticides using *in vitro* enzymatic inhibition assays, *Toxics* 10 (8) (2022) 448.
- [60] T. Čadež, D. Kolić, G. Šinko, Z. Kovarik, Assessment of four organophosphorus pesticides as inhibitors of human acetylcholinesterase and butyrylcholinesterase, *Sci. Rep.* 11 (1) (2021) 1–11.
- [61] G. Kaur, A.K. Jain, S. Singh, CYP/PON genetic variations as determinant of organophosphate pesticides toxicity, *J. Genet.* 96 (1) (2017) 187–201.
- [62] B. Clothier, M.K. Johnson, E. Reiner, Interaction of some trialkyl phosphorothiolates with acetylcholinesterase. Characterization of inhibition, aging and reactivation, *Biochim. Biophys. Acta* 660 (2) (1981) 306–316.
- [63] A. Miličević, G. Šinko, Use of connectivity index and simple topological parameters for estimating the inhibition potency of acetylcholinesterase, *Saudi Pharmaceut. J.* 30 (4) (2022) 369–376.
- [64] H. Zhao, J. Hu, Total residue levels and risk assessment of flufenacet and its four metabolites in corn, *J. Food Compos. Anal.* 106 (2022), 104268.
- [65] J. Egea, I. Fabregat, Y.M. Frapart, P. Ghezzi, A. Görlich, T. Kietzmann, et al., European contribution to the study of ROS: a summary of the findings and prospects for the future from the COST action BM1203 (EU-ROS), *Redox Biol.* 13 (2017) 94–162.
- [66] P. Rytczak, A. Drzazga, E. Gendaszewska-Darmach, A. Okruszek, The chemical synthesis and cytotoxicity of new sulfur analogues of 2-methoxy-lysophosphatidylcholine, *Bioorg. Med. Chem. Lett* 23 (24) (2013) 6794–6798.
- [67] P.G. Layer, Cholinesterases preceding major tracts in vertebrate neurogenesis, *Bioessays* 12 (9) (1990 Sep) 415–420.
- [68] C.N. Pope, S. Brimijoin, Cholinesterases and the fine line between poison and remedy, *Biochem. Pharmacol.* 153 (2018) 205–216.
- [69] G. Viswanath, S. Chatterjee, S. Dabral, S.R. Nanguneri, G. Divya, P. Roy, Anti-androgenic endocrine disrupting activities of chlorpyrifos and piperophos, *J. Steroid Biochem. Mol. Biol.* 120 (1) (2010) 22–29.
- [70] G. Lemaire, W. Mnif, J.M. Pascussi, A. Pillon, F. Rabenoelina, H. Fenet, et al., Identification of new human pregnane X receptor ligands among pesticides using a stable reporter cell system, *Toxicol. Sci.* 91 (2) (2006) 501–509.
- [71] M.A. Martínez, J.L. Rodríguez, B. Lopez-Torres, M. Martínez, M.R. Martínez-Larrañaga, J.E. Maximiliano, et al., Use of human neuroblastoma SH-SY5Y cells to evaluate glyphosate-induced effects on oxidative stress, neuronal development and cell death signaling pathways, *Environ. Int.* 135 (2020), 105414.
- [72] M. Arena, D. Auteri, S. Barmaz, G. Bellisai, A. Brancato, D. Brocca, et al., Peer review of the pesticide risk assessment of the active substance phenmedipham, *EFSA J.* 16 (1) (2018), e05151.
- [73] M. Arena, D. Auteri, S. Barmaz, G. Bellisai, A. Brancato, D. Brocca, et al., Peer review of the pesticide risk assessment of the active substance desmedipham, *EFSA J.* 16 (1) (2018), e05150.